Solar-Driven Thermochemical Production of Sustainable Liquid Fuels from H_2O and CO_2 in a Heliostat Field

Manuel Romero[1], José González-Aguilar[1], Andreas Sizmann[2], Valentin Batteiger[2], Christoph Falter[2], Aldo Steinfeld[3], Stefan Zoller[3], Stefan Brendelberger[4], Dick Lieftink[5]

[1] IMDEA Energy Institute, Avda. Ramón de la Sagra 3, 28935 Móstoles, Spain

[2] Bauhaus Luftfahrt, Willy-Messerschmitt-Straße 1, 82024 Taufkirchen, Germany

[3] ETH Zürich, Sonneggstr Zürich, Switzerland

[4] German Aerospace Center (DLR), Linder Höhe, 51147 Cologne, Germany

[5] HyGear, P.O. Box 5280, 6802 EG Arnhem, The Netherlands

Abstract

The technology presented, Sunlight to Liquid or StL, has as main achievement the demonstration, for the first time, of a fully integrated system producing liquid fuels from concentrated sunlight, water and carbon dioxide under real on-sun conditions provided by a modular heliostat field and therefore promoting the StL technology to a readiness level (TRL) of 5. The main objective driving this development is the decarbonization of transport sector, with particular emphasis on aviation. For this purpose, a solar fuel research facility comprising a high-flux solar concentrating heliostat field and tower, a solar thermochemical reactor system, and a gas-to-liquid conversion plant have been installed at a sunny site in Móstoles, Spain. Ceria is used as the reactive material in the solar reactor, which undergoes a temperature and pressure swing in a redox cycle, splitting water and carbon dioxide into hydrogen and carbon monoxide. This synthesis gas is then converted into hydrocarbons downstream via a Fischer-Tropsch conversion plant. The customized heliostat field has been able to provide irradiances above 3000 kW/m^2 onto the small aperture of the 50kW solar reactor, producing up to 150 L/h solar syngas subsequently converted into liquid fuel.

Keywords: Solar Fuels, Sunlight-to-Liquid, CSP, Central Receiver Systems, Solar Thermochemical Conversion

1. Introduction

Aviation has a rising share of its CO_2 emissions due to its continued high growth rates on the order of 5% in recent years (ICAO, 2016). At this strong growth, the currently achieved reductions in annual specific fuel burn of 1.5% due to technical advancement are not enough to reduce or even stabilize the emissions over time. Unlike for cars, the aircraft is very weight sensitive, which poses strict requirements on its energy storage. It is expected that long-range air travel is going to rely on hydrocarbon fuels even in the future due to the high demand on energy density of the batteries for these missions. Nevertheless, the aviation industry has set itself quite demanding targets with respect to a reduction of its CO_2 emissions. In its Strategic Research and Innovation Agenda for year 2050 the Advisory Council for Aviation Research and Innovation in Europe-ACARE establishes a goal of CO_2 emissions per passenger kilometer to be reduced by 75% and NOx emission by 90% all relative to the year 2000 (ACARE, 2017). Similarly, in scenarios proposed by Air Transport Action Group-ATAG, beginning from the year 2020, a carbon-neutral growth is targeted and for the year 2050, a reduction to 50% with respect to the year 2005. Improvements of current technology, air traffic management and infrastructure use is not able to reduce the emissions from the growing aviation sector therefore the use of alternative fuels with lower specific CO_2 emissions than conventional fuel is required. Heavy duty trucks, maritime and road transportation are also expected to rely strongly on liquid hydrocarbon fuels. Thus, the large volume availability of 'drop-in' capable renewable fuels is of great importance for decarbonizing the transport sector.

doi:10.18086/swc.2019.23.02 Available at http://proceedings.ises.org

In recent years, significant progress has been accomplished in the development of CSP (Concentrating Solar Power) systems making use of heliostat fields, with central receivers on top of a tower, capable of achieving irradiances well above 2000kW/m^2. Such high solar radiation fluxes allow the conversion of solar energy to thermal reservoirs well beyond 1000ºC, which are needed for the more efficient two-step thermochemical cycles using metal oxide redox reactions, either for use in thermochemical energy storage (Carrillo et al., 2019) or for the production of solar fuels (Romero and Steinfeld, 2012). The H_2O/CO_2-splitting redox cycle can be represented by:

1st step, reduction $$MO_{ox} \rightarrow MO_{red} + \frac{1}{2} O_2 \quad \text{(eq. 1)}$$

2nd step, oxidation $$MO_{red} + H_2O \rightarrow MO_{ox} + H_2 \quad \text{(eq. 2)}$$

$$MO_{red} + CO_2 \rightarrow MO_{ox} + CO \quad \text{(eq. 3)}$$

The first, endothermic step is the solar thermal reduction of the metal oxide MO_{ox} to the metal or the lower-valence metal oxide MO_{red}. The second, non-solar, exothermic step is the reaction of the reduced metal oxide with H_2O or CO_2 to form H_2 or CO, and reform the original metal oxide which is recycled to the first step. The net reaction is $H_2O = H_2 + 0.5O_2$, but since H_2 and O_2 are formed in different steps, the need for high-temperature gas separation is thereby eliminated. The second step can be accomplished on demand at the fuel consumer site, as it is decoupled from the availability of solar energy. CO_2 and H_2O can be co-fed to produce synthesis gas (syngas), the building block for a wide variety of synthetic fuels including Fischer-Tropsch liquid hydrocarbon fuels. Following that approach, the project herewith reported, SUN-to-LIQUID (http://www.sun-to-liquid.eu/), establishes a non-biomass non-fossil path to synthesize renewable liquid hydrocarbon fuels via a thermochemical redox cycle, which inherently operates at high temperatures and utilizes the full solar spectrum (Figure 1). Thereby, it provides a thermodynamically favorable path to solar fuel production with the potential of high energy conversion efficiency and, consequently, economic competitiveness.

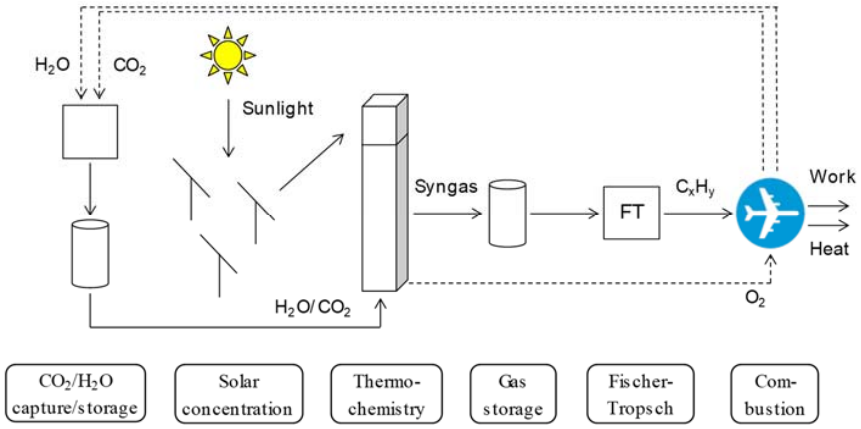

Fig. 1: Integrated solar thermochemical fuel production with a Fischer-Tropsch process for production of aviation fuel.

Current biofuel technology does not meet sustainability and availability requirements at the scale of future global fuel demand (Mohr and Raman, 2013), therefore the implementation of other renewables-to-liquids routes should become a priority in the years to come. Using solar concentrating systems and thermochemical conversion routes is one of the StL (Sunlight-to-Liquid) options with huge untapped potential. Solar fuels are most efficiently and competitively produced in desert regions with high solar irradiation (typically > 2000 kWh/m^2 per year), thus there is no land competition with food or feed production. In contrast to current alternative fuels, solar fuels can easily meet future fuel demand by utilizing less than 1% of the global arid and semi-arid land. In the case of StL, the water footprint consists of 7.4 liters per liter of jet fuel of direct demand on-site and the area-specific productivity is found to be 33,362 liters per hectare per year of jet fuel equivalents, where the land coverage is

mainly due to the concentration of solar energy for heat and electricity. The water footprint and the land requirement of the solar thermochemical fuel pathway are larger than the best power-to-liquid pathways but an order of magnitude lower than the best biomass-to-liquid pathways (Falter and Pitz-Paal, 2017). For the case of a solar tower concentrator with CO_2 capture from air, jet fuel production costs of 2.23 €/L and life cycle greenhouse gas (LC GHG) emissions of 0.49 kgCO2-equiv/L are estimated (Falter et al., 2016).

2. Project Technical Description

The SUN-to-LIQUID project is comprised of leading European research partners, namely Bauhaus Luftfahrt (Coordinator), ETH Zurich, IMDEA Energy, DLR, HyGear, Abengoa Energía and ARTTIC. An overview of the experimental facility is shown in Fig. 2 (Koepf et al., 2019). A solar-driven thermochemical reactor based on ceria RPC (Reticulated Porous Ceramics) structures is mounted in a 15 m high tower in the west operating position; in the east operating position, a water calorimeter is positioned. Concentrated solar power is delivered by 169 heliostats with a 3 m^2 facet area and two focal lengths created by two axes of curvature. A photometric power delivery measurement system calibrated with a heat flux gauge and a 50 kW water calorimeter is installed in front of the solar receivers, and a modular Fisher-Tropsch (FT) catalytic processing plant to produce long-chain hydrocarbon fuels from the solar syngas is placed at the base of the tower. Syngas is delivered at ambient pressure from the solar reactor in the tower and compressed in two stages inside the FT system. The heliostat field, which is operated from the control room, was developed by IMDEA Energy in Spain. The solar reactor and water calorimeter, which are placed at the top of the tower on the experimental level but also operated from the control room, were developed by ETH Zurich in Switzerland. The flux measurement acquisition system (FMAS), which moves in front of both receivers in the tower, was developed by DLR in Germany, and the gas-to-liquid (GtL) facility was developed by HyGear in the Netherlands. The entire facility is situated on a 50 x 50 meter plot of land. The pilot plant is capable of operation year round; the solar concentration system is designed to deliver an average of 2,500 kW/m^2 (50 kW into an aperture diameter of 16 cm) even in December. The solar reactor is designed such that operation (although not with high efficiency) is possible with less than nominal power, and the gas-to-liquid system has multiple stages of syngas compression and buffer tanks. In addition to optimizing on-sun solar reactor operation and demonstrating high solar-to-fuel energy conversion efficiency, a major project priority is to demonstrate the long-term operation of the fully integrated facility.

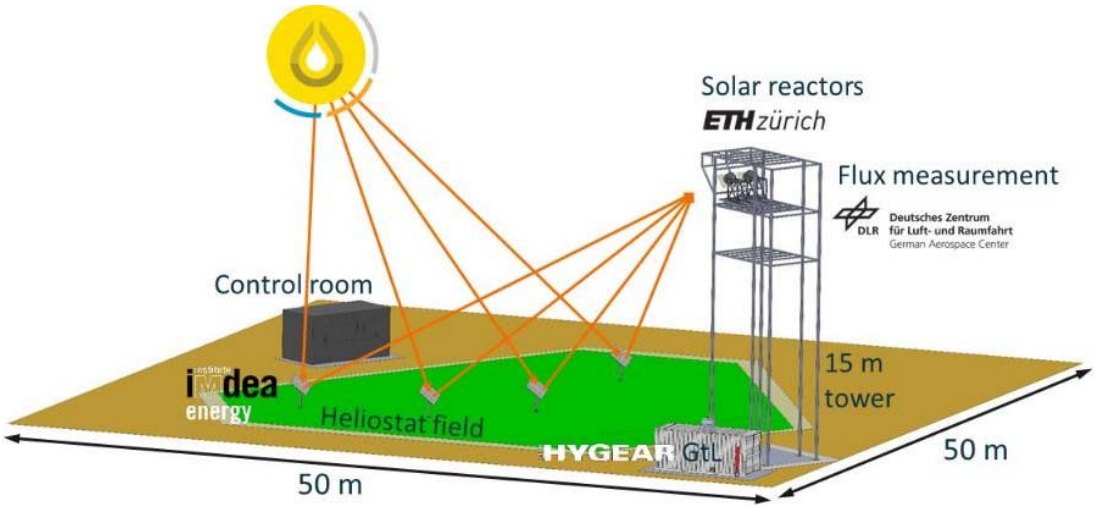

Fig. 2: Sketch of the experimental facility. Key system components are the solar concentration system comprising a heliostat field and a solar tower (IMDEA Energy), the solar reactors, which are placed at the top of the tower (ETHZ), the flux measurement system in front of the receivers in the tower (DLR), and the gas-to-liquid facility which is placed at the bottom of the tower (HyGear). The integrated plant is operated from the control room. The entire facility is situated on a 50 x 50 meter plot of land. Optical height of the tower is 15 m.

2.1. Design and construction of solar field

The high-flux solar concentration system has been explicitly designed according to the specifications and requirements of the SUN-to-LIQUID project. According to the technical specifications it was required to provide 50 kW onto reactor surface of only 16 cm diameter, allowing it to reach temperatures in excess of 1500 ºC. The small size of the reactor aperture and the required irradiance (2500 kW/m^2 average on aperture), were challenging for a heliostat field with very small power (tentatively few-hundred kWth). Initially it was uncertain whether such a small heliostat field with the intrinsic cosine factor limitations of any off-axis solar concentrator would be able to reach the required specifications. IMDEA Energy performed an initial feasibility design study and based on a ray-tracing analysis it was shown that a dense ultra-modular field could achieve an optical performance comparable to parabolic dishes or solar furnaces with secondary concentration optics (Romero et al., 2017). The sensitivity analysis for a small field of 500kW, as shown in Figure 3, revealed that it was possible to reach solar field optical efficiency about 80% for a solar concentration factor of 2000x and about 71% for 3000x, however the mirror field should be highly packed, with a density > 35% (ratio between mirrors area and land occupied by the heliostat field). The positive impact of density on optical efficiency is because of the drastic reduction of spillage on reactor aperture at solar concentrations above 2000x. A higher density would be required for a smaller solar field and higher concentrations factors. On the contrary, a SoA (State of the Art) solar field with a typical density of 23% would lead to 10% lower optical efficiency. A similar analysis regarding the influence of heliostat unitary size revealed the need of using small units of less than 5 m^2 and with short focal lengths to optimize the peak onto aperture.

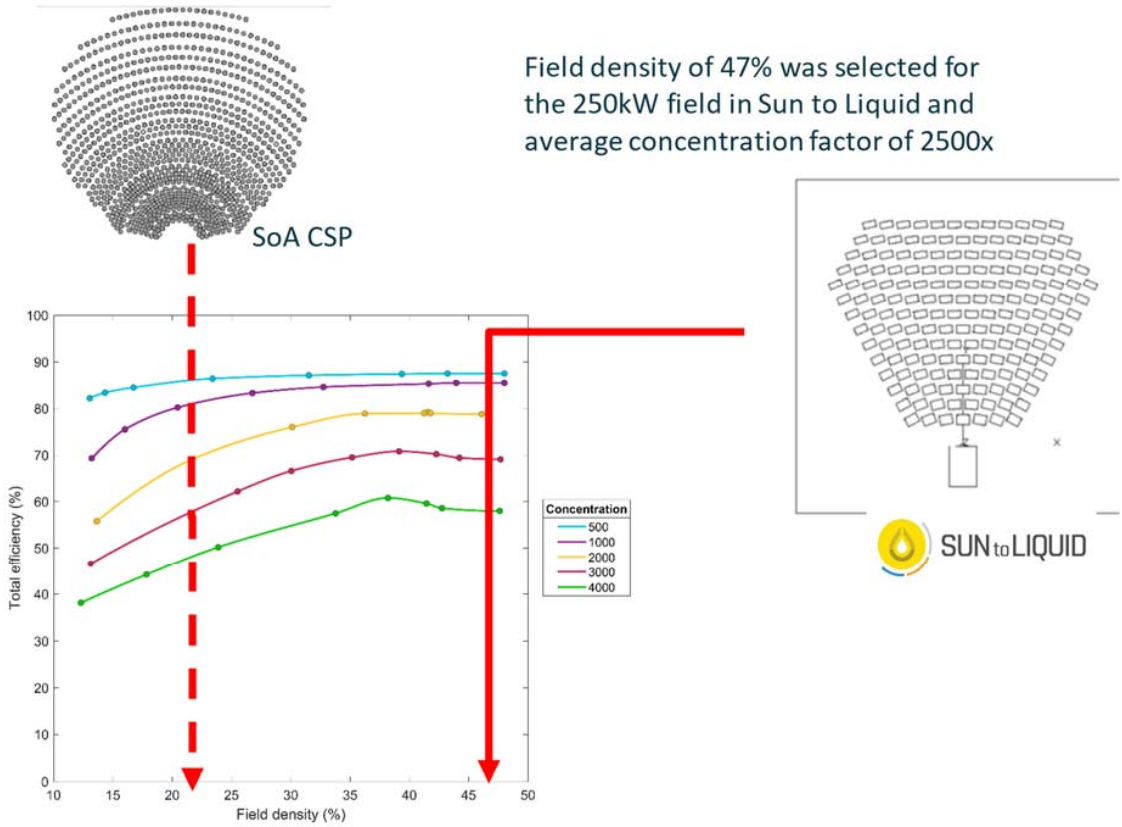

Fig. 3: Analysis on the impact of solar field density on optical efficiency for a small plant of 500kW at different concentration ratios.

Based on the previous information, eventually a 250kW heliostat field has been designed with 169 small-area heliostats (3 m^2 each) and with a short focal length arranged in 14 rows at close distance to a solar tower of only 15 m optical height to provide the required 50 kW onto reactor surface. The heliostat field has a cornfield layout as shown below. A detailed ray tracing analysis has been carried out for spring equinox, summer, and winter solstice, including the shadowing effect of the tower. The use of two focal lengths (20 m and 30 m) offers a significant increment in peak fluxes. The optimum value was obtained for a design where rows 1 to 8 have facets of 20 m of focal length, and rows 9 to 14 facets of 30 m of focal length. This is the option finally adopted for the SUN-to-LIQUID to guarantee high solar flux throughout the entire year (Romero et al., 2017). The row and azimuthal spacing between the single facet heliostats are 2.25 and 2.60 m respectively and the distance from the tower to the first row of heliostats only 4 m. The last row is 33.25 m away from the tower. Compared to the 500kW example shown in Figure 3, the 250kW heliostat field for a concentration ratio of 2500x finally required a higher density of about 47%.

Fig. 4: (Left) Aerial view of the heliostat field from top of the tower. Control room at the rear. (Right) Lateral view of single heliostat of 3m^2 reflecting surface and two rectilinear actuators.

Heliostat assembly makes use of shaft motors and tracker structure from the ST44M2HEL3 model of Sat Control d.o.o.. Some technical characteristics of the heliostat are: Pedestal pole of 1.4 m height; Azimuthal angle range: 100º; Elevation angle range: from 20º to 90º, corresponding 90º to horizontal stow position with mirror facing to zenith; Turning speed of azimuthal and elevation angle shafts less than 0.1º/s; Tracking accuracy: less than 0.1º. Conventional facets supplied to commercial plants are making use of cold mechanical conformation techniques with supporting frames and very long focal lengths (hundreds of meters). However, an ultra-modular solar field requires approximately 10 times that level of deformation. Because of that, a specific development for facet manufacturing with cold mechanical bending has been tested in collaboration with the company Rioglass Solar. The light design makes use of high reflectivity mirrors (of 3 mm thickness) bonded to vertical thin plates and pre-conformed by gravity sagging onto a master model. The mirror dimensions and technical specifications are as follows: Dimensions: 1605 x 1900 mm x 3 mm; Fresh reflectivity: 94.3% average. The beam quality of the heliostats (once excluded sunshape) is average 2.5 mrad. The construction of the solar field was completed in February 2017.

2.2. Measurement of solar flux concentration

The camera-based flux measurement system (FMAS) was designed by DLR to measure the solar flux profile in front of the reactor with minimal interruption of the actual reactor operation (Thelen et al., 2017). The measurement plane is flat and inclined 40º in the same way as the solar reactor. The target of the FMAS system is coated with a diffuse reflecting aluminium oxide coating, welded cooling channels at the back side ensure proper cooling during measurement on sun. The target also incorporates a Gardon radiometer (Seqoia Technology) to calibrate the flux distribution against the Gardon radiometer reading at one measurement point. This arrangement can be moved quickly and precisely in front of the apertures (Figure 5), the overall interruption of reactor operation due to a flux measurement can be as short as ten seconds. Further integral components of the

FMAS system are a camera system[1] to record diffuse reflection from the target, which is installed in a housing just next to the control room. A measurement software determines the solar flux distribution at the measurement plane, as a next step the solar radiative power at the aperture of the receiver is inferred from a ray-tracing simulation of the heliostat field. The measurement accuracy of the FMAS system has been tested against a direct power measurement using a water calorimeter designed and implemented by ETHZ and IMDEA Energy. From these measurements it was concluded that a direct power measurement using the water calorimeter permanently installed at one experimental position, in combination with FMAS measurements, both in front of the water calorimeter and the solar reactor, provide the most accurate quantification of the solar power at the solar reactor aperture plane. The FMAS system was installed at the experimental platform in spring 2017 and it was quickly recognized as a useful tool for the calibration of single heliostats and for the improvement of the field operation in general.

Fig. 5: Left: Technical drawing of the flux measurement system (in blue) in front of one of the receivers. Right: Installation of the flux measurement system at the experimental level of the solar tower (solar reactors not yet installed). The rail at the bottom allows to move the flux measurement system quickly in-between the apertures and into a safe position, the cooling water supply is visible.

Regarding the water calorimeter, the vessel, aperture and mounting position mimic the solar reactor to derive solar radiative power at the reactor aperture from representative caloric measurements. Because the front section of the vessel, including window and cavity aperture, are exactly the same as that used for the solar reactor, power delivery calibration by this method is extremely accurate. The calorimeter cavity, is comprised of approximately 20 meters of coiled copper tubing and coated with a high emissivity enamel. The calorimeter cavity has a diameter (350 mm) and length (250 mm) also closely matching that of the solar reactor. The calorimeter is equipped with a highly accurate water flow meter and thermocouples at the inlet and outlet of the water lines. The final strategy for the power measurements is shown Figure 6. The water calorimeter is installed at one window (east side) of the experimental level, the solar reactor is installed at the other window (west). The FMAS system measures the flux distribution in front of both apertures. The approach to map the accuracy of the water calorimeter measurement to the FMAS power measurement in front of the solar reactor is explained in Figure 7 by a representative measurement sequence (Koepf et al., 2019).

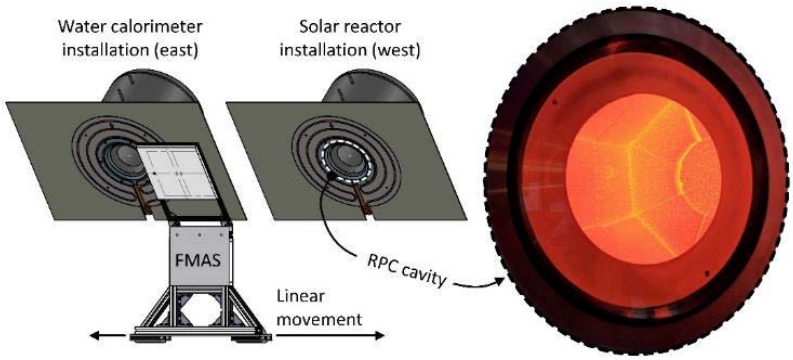

[1] Camera: Allied Vision Technologies Prosilica GT 1930L mono, Tele objective: Tamron SP 150-600 EF-mount

Fig. 6: Final design philosophy for power measurements. The water calorimeter is installed at the east window of the experimental platform; the solar reactor is installed at the west window. The FMAS system measures the flux distribution both in front of the water calorimeter and in front of the solar reactor. This approach maps the accuracy of the water calorimeter measurement to the FMAS measurement in front of the solar reactor.

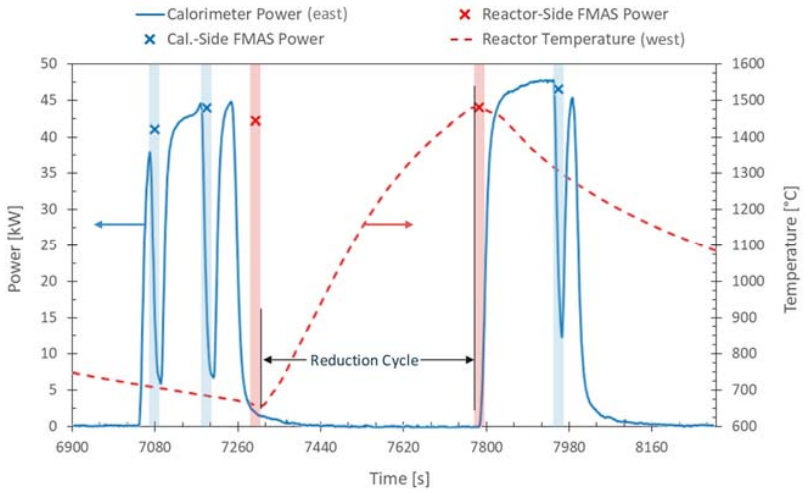

Fig. 7: Representative measurement cycle to deduce the solar radiative power at the aperture of the solar reactor. The solar reactor cavity temperature is shown in dashed red (right axis), along with water calorimeter measurements in blue (left axis) and FMAS measurements. FMAS measurements in front of the water calorimeter and the solar reactor are indicated in blue and red respectively. The combination of these measurements determines the solar power entering the reactor during the reduction cycle, which is not easily accessible for direct measurement.

2.3. Solar reactor

A review summarizes state-of-the-art metal oxide redox materials and discusses advantages and disadvantages of both stoichiometric (i.e. iron oxide based cycles) and nonstoichiometric (i.e. ceria based cycles) materials in the context of thermodynamics, chemical kinetics, and material stability (Scheffe and Steinfeld, 2014). Non-stoichiometic cerium oxide (ceria) has emerged as an attractive redox active material because of its high oxygen ion conductivity and cyclability, while maintaining its fluorite-type structure and phase (Chueh et al., 2010). Thermodynamic analysis indicate the potential of reaching $\eta_{\text{solar-to-fuel}} = 20\%$ in the absence of heat recovery, and exceeding 30% by recovering the sensible heat of the hot products. The use of CeO_2 and its non-stoichiometric reduction/oxidation in thermochemical cycling is depicted in Figure 8. In the previous European project SOLAR-JET http://www.solar-jet.aero a total of 291 stable redox cycles were performed by ETHZ in a 4kW reactor with a solar simulator, yielding 700 standard liters of high-quality syngas, which was compressed and further processed via Fischer-Tropsch synthesis to a mixture of naphtha, gasoil, and kerosene (Marxer et al., 2015).

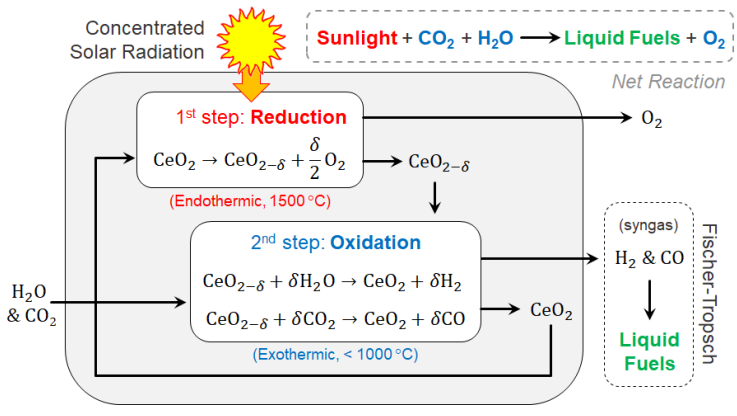

Fig. 8: The Ceria Thermochemical Redox Cycle for solar syngas production.

It was shown by previous experiments on ceria bricks and ceria felt that the reduction step is limited by heat transfer to the ceria structure (Furler et al., 2012; Marxer et al., 2017) and the oxidation step by the available surface area. Ceria is thus used as a reticulated porous ceramic (RPC) with different scales of porosity. On a larger scale in the mm-range, holes in the ceria structure reduce the optical thickness of the material and thus permit

efficient heating by volumetric absorption of concentrated solar radiation. In Figure 9 it is depicted a cross section of the SUN-to-LIQUID 50kW reactor based on RPC ceria structure with dual-scale porosity located inside the cavity.

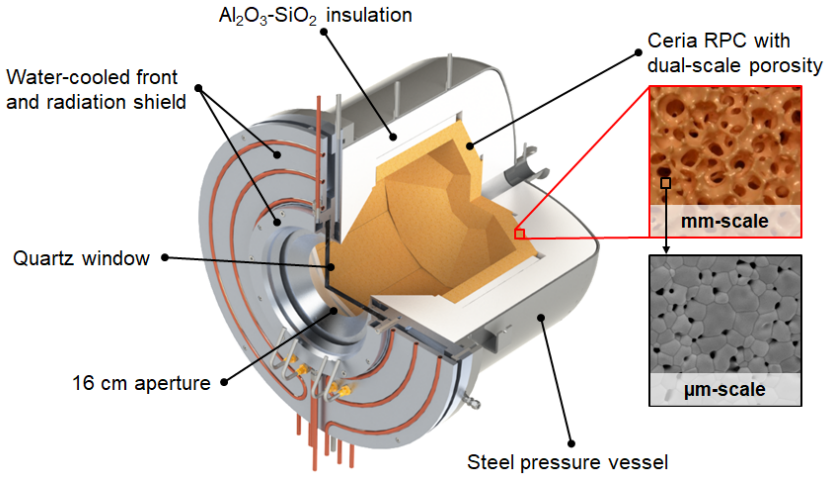

Fig.9: Overview of the Solar Reactor Design

The current design has been developed by ETH Zurich based on their experience with previous materials and represents the most efficient design nowadays to absorb concentrated radiation. The splitting of water and carbon dioxide can be performed most efficiently using a material with a large surface area because the overall reactions are limited by the oxygen exchange reactions on the surface (Furler et al., 2017). On a microscopic scale, the material thus has pores that increase the specific surface area to enhance the kinetics of the oxidation step. The combination of both porosities on different length scales therefore allows for an efficient redox cycle which is composed of quick heating and fast reoxidation kinetics. The reactor has been tested in a solar simulator at a power level of 30 kW prior to its shipment to the solar thermochemical plant in Móstoles in summer 2018.

2.4. Gas-to-Liquid Plant

The syngas coming from the solar reactor is converted into liquid hydrocarbons in a gas-to-liquids subsystem located next to the solar tower. The GTL plant comprises three modules: preparation module; generation module and steam reforming module.

In the preparation module the gas is received from the solar reactor and from the steam reformer module. First the gas is dried by a cooling/ condensation system and second by an adsorption bed filled with silica. The dried gas is subsequently compressed and stored in a gas bottle at a maximum pressure of 130 bar. Condensate is removed by water separators and drained. When the buffer is filled with H_2 and CO at a pressure over 100 bar the gas is taken form the bottle and depressurized to 20 bar and fed to the Fischer –Tropsch reactor. This reactor is a multi-tubular reactor containing a Co-based catalyst (Figure 10). The catalyst is heated to about 210°C by a system in which thermal oil is heated and pumped in an annular space around the catalytic reactor. The syngas is then reacted to liquid hydrocarbons via the Fischer-Tropsch process, the simplified net reaction of which is:

$$(2n)H_2 + nCO \longleftrightarrow -(CH_2)_n - + nH_2O. \qquad \text{(eq. 4)}$$

These reaction conditions correspond to a chain-growth probability in a range of $\alpha = 0.85 \ldots 0.9$ and resembles at small scale the typical operation conditions of commercial GtL plants for synthetic diesel and jet fuel production. The resulting FT hydrocarbons contain mainly waxes (>C22) and liquid hydrocarbons (C5-C21), but also a significant fraction of gaseous hydrocarbons (C1-C4). All products from the FT reactor enter the product separation tank in a gaseous or liquid phase. First waxy species are separated at a temperature of about 80°C, the separation of liquid products (hydrocarbons and water) from the tail gas takes place in a second step at room temperature. The gaseous species are then sent to the reforming unit. The SUN-to-LIQUID gas-to-liquid subsystem is installed on-site in a standard-size container (Figure 11).

Fig. 10: Main conversion modules in the SUN-to-LIQUID GtL container. Left to right: Fischer-Tropsch reactor tubes, product separation vessel, steam reformer (in opened position) to recycle gaseous hydrocarbons into syngas.

Fig. 11: Heliostat field with 169 heliostats focusing onto solar reactor with ceria located on top of a 15-m tower (optical height). On the right side at ground level the container with the gas-to-liquid conversion plant.

3. Results

Early testing in 2018 was dedicated to confirm the performance of the heliostat field according to the challenging specifications in terms of irradiance onto aperture and also in terms of stable supply of power for extended periods of more than six hours required for the daily campaigns of cycles. A refined methodology was developed involving the characterization of individual pointing calibration map of each heliostat. These empirically determined inclination maps allowed to improve the aiming precisions and tracking accuracies by approximately one order of magnitude. The further improvement of the tracking accuracy enabled the delivery of power levels well above

50 kW to the solar reactor aperture in the summer of 2018 (see Figure 12). For the test presented, the total power inside the 16-cm reactor aperture was 71.53 kW and 259 kW onto the whole FMAS target of 34x34cm. Peak flux registered was more than 4000 kW/m^2 and well above 2500 kW/m^2 at all points of reactor aperture. In the following the solar reactor system could be commissioned and put into routine operation.

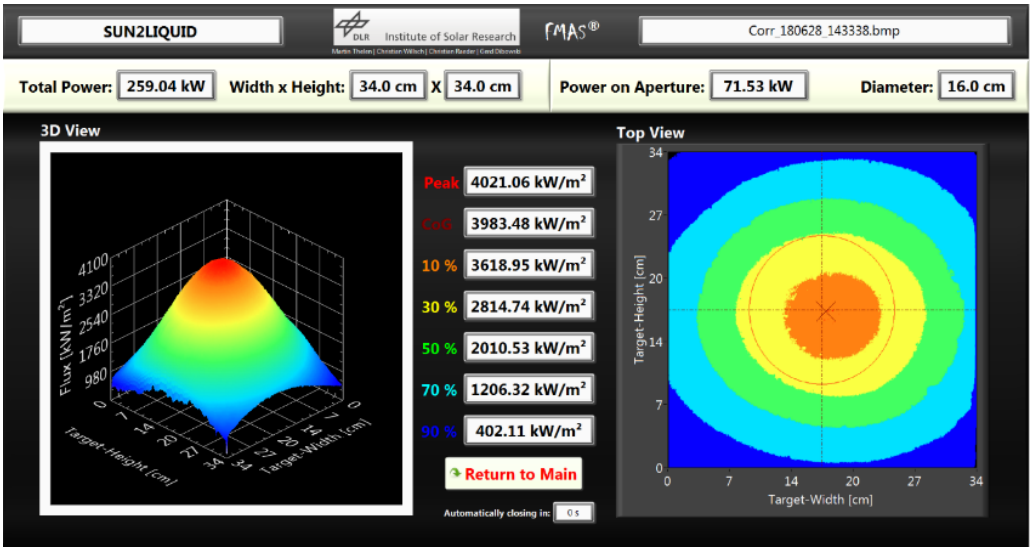

Fig. 12: Power measurement well above 50 kW, 15 minutes behind solar noon on 28th June 2018, for a DNI of approximately 800 W/m2 with the FMAS system.

Typical daily operation of the solar reactor is represented in Figure 13. With a reduced number of heliostats, a smooth pre-heating from ambient temperature to 1000ºC is carried out. Once temperature is reached, a pre-cycle is done raising temperature up to 1500ºC by means of a gradual ramp of power followed by cooling step. After this process the routine cycling of the reactor follows from 800 to 1500ºC. Heating cycles corresponding to reduction step were carried in 12 minutes for 30kW tests and reduced to less than 8 minutes for 50kW of incident power on the aperture. Temperature decrease was obtained by natural cooling in periods of 30-minutes. In a typical sunny day an average of 8 active cycles were carried out. Shutting down was then completed with a smooth cooling-down process to protect the reactor components. Figure 14 show a front view of water calorimeter on the east side and solar reactor emitting IR radiation during oxidation step (cooling down) on the west side.

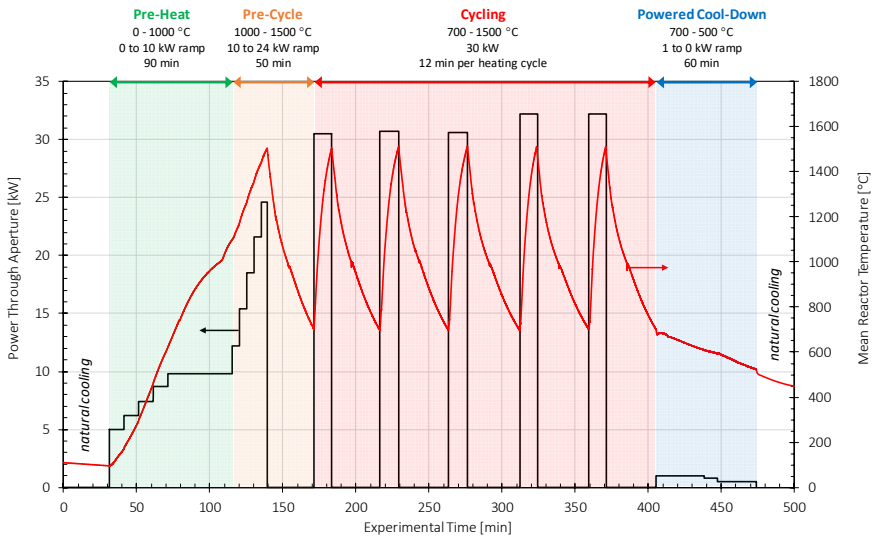

Fig. 13: Typical operation strategy of solar reactor including pre-heating, pre-cycle, routine redox cycling and cooling down.

Fig. 14: Right- Solar reactor emitting radiation during oxidation step and cooling down. Left – Calorimetric analogue of solar reactor for confirmation of incident power during testing.

After a first testing campaign dedicated to optimize the operational conditions to obtain a high quality syngas, in April 2019 it was successfully demonstrated the production of syngas with a molar ratio H_2:CO = 2, suitable for FT-synthesis. It was also demonstrated that typically 7-10 cycles can be carried out per day depending on the direct normal irradiation. In these cycles, the reduction is performed at temperatures up to 1500 °C and vacuum pressures down to 10 mbar while the oxidation is performed at temperatures below 900 °C and 1 atm total pressure.

During the months of June-July 2019 the operation of fully integrated system has been achieved with on-sun routine operation. As many as 100 cycles since June 2019 have produced syngas, in some cases in fully sunny days with operation from 9 am till 6 pm and some other days partially cloudy and with transients. With an average of solar syngas produced of 100-150 liters per cycle, more than 10,000 liters of solar syngas have been pressurized and processed by the FT reactor. The solar syngas contains CO, H_2 and unreacted CO_2 as the only constituents.

Each pulse during oxidation phase consists of about 100 -150 liters of solar gas, increasing the buffer pressure about 1.2-2 bar at the GtL plant. After June 6 the solar gas stored in the buffer was used to run the Fischer-Tropsch reactor. The system has run at 20 bar and a temperature up to 210°C and a flow of 6 slm of solar syngas. After the first campaign in summer 2019, the production of liquid fraction of Fischer-Tropsch product from 100% solar syngas was successfully demonstrated though still analysis of the composition is not available at the time of writing.

4. Conclusions and outlook

The SUN-to-LIQUID consortium developed a demonstration facility for the production of solar thermochemical liquid fuels. The high-flux solar plant has been built at the site of IMDEA Energy in Móstoles, Spain. The fully integrated system comprising high-flux solar concentration field, 50kW solar reactor and down-scaled GtL plant to process 6 slm of syngas has been successfully commissioned, characterized and operated on a routine basis.

In summary, the main goals of the long-term experimental campaign were achieved. The stable cyclic operation of the solar reactor was shown in multiple consecutive redox cycles. High-quality syngas suitable for FT synthesis was produced with total selectivity by simultaneous co-splitting of H_2O and CO_2. The technical feasibility of the complete 50 kW solar reactor system was demonstrated in a solar tower optical configuration and integrated with the FT synthesis unit.

The further scale-up of the technology could provide, on a large scale, solar fuels with considerably reduced CO_2 emissions over their life cycle compared to conventional fuels.

5. Acknowledgments

The SUN-to-LIQUID Project has received funding from the European Union's Horizon 2020 research and innovation programme under grant agreement No 654408. This work was supported by the Swiss State Secretariat for Education, Research and Innovation (SERI) under contract number 15.0330. This document reflects the authors' view only and the INEA must not be taken as responsible for any use that may be made of the information it contains.

6. References

ACARE 2017 Update Volume 1. Strategic Research and Innovation Agenda. Available at https://www.acare4europe.org/documents/delivering-europe's-vision-aviation-sria-2017-update

Carrillo, A.J. González-Aguilar, J., Romero, M., Coronado J.M., 2019. Solar Energy on Demand: A Review on High Temperature Thermochemical Heat Storage Systems and Materials. Chem. Rev. 119, 4777−4816

Chueh, W. C., Falter, C., Abbott, M., Scipio, D., Furler, P., Haile, S. M., and Steinfeld, A., 2010, "High-flux solar-driven thermochemical dissociation of CO2 and H2O using nonstoichiometric ceria.," Science, 330(6012), pp. 1797–1801.

Falter, C., Batteiger, V., Sizmann, A., 2016. Climate Impact and Economic Feasibility of Solar Thermochemical Jet Fuel Production, Environ. Sci. Technol., 50,1, 470-477

Falter, C., Pitz-Paal, R., 2017. Water Footprint and Land Requirement of Solar Thermochemical Jet-Fuel Production. Environ. Sci. Technol., 51, 21, 12938-12947.

Furler, P., Marxer, D., Scheffe, J., Reinalda, D., Geerlings, H., Falter, C., Batteiger, V., Sizmann, A., and Steinfeld, A., 2017, "Solar kerosene from H2O and CO2," AIP Conf. Proc., 1850. 100006.

Furler, P., Scheffe, J., Gorbar, M., Moes, L., Vogt, U., and Steinfeld, A., 2012, "Solar thermochemical CO2 splitting utilizing a reticulated porous ceria redox system," Energy and Fuels, 26(11), pp. 7051–7059.

ICAO 2016: ref. 20160000_REP_ICAO Environmental Report 2016_p16-22

Koepf, E., Zoller, S., Luque, S., Thelen, M., Brendelberger, S., González-Aguilar, J., Romero, M., Steinfeld, A., 2019. Liquid fuels from concentrated sunlight: An overview on development and integration of a 50 kW solar thermochemical reactor and high concentration solar field for the SUN-to-LIQUID project. AIP Conference Proceedings 2126, 180012.

Thelen, M., Raeder, C., Willsch, C., Dibowski, G. 2017 A high-resolution optical measurement system for rapid acquisition of radiation flux density maps. AIP Conference Proceedings 1850, 150005.

Marxer, D. A., Furler, P., Scheffe, J. R., Geerlings, H., Falter, C., Batteiger, V., Sizmann, A., and Steinfeld, A., 2015, "Demonstration of the entire production chain to renewable kerosene via solar-thermochemical splitting of H2O and CO2," Energy & Fuels, 29(5), pp. 3241–3250.

Marxer, D., Furler, P., Takacs, M., and Steinfeld, A., 2017, "Solar thermochemical splitting of CO2 into separate streams of CO and O2 with high selectivity, stability, conversion, and efficiency," Energy Environ. Sci., 10(5), pp. 1142–1149.

Mohr, A., Raman, S., 2013. Lessons from first generation biofuels and implications for the sustainability appraisal of second generation biofuels. Energy Policy 63, 114.

Romero, M., González-Aguilar, J., Luque, S., 2017. Ultra-modular 500m2 heliostat field for high flux/high temperature solar-driven processes. AIP Conference Proceedings, 1850, 030044-1/9.

Romero, M., Steinfeld, A., 2012. Concentrating Solar Thermal Power and Thermochemical Fuels, Energy Environ. Science, **5**, 9234.

Scheffe, J.R., Steinfeld, A., 2014. Oxygen Exchange Materials for Solar Thermochemical Splitting of H2O and CO2 – A Review, Materials Today 17, 341.